Front. Phys. 11(6), 114214 (2016)
DOI 10.1007/s11467-016-0606-1

REVIEW ARTICLE

Review of LIBS application in nuclear fusion technology

Cong Li (李聪)[1], **Chun-Lei Feng** (冯春雷)[1], **Hassan Yousefi Oderji**[1], **Guang-Nan Luo** (罗广南)[2], **Hong-Bin Ding** (丁洪斌)[1,†]

[1] *Key Laboratory of Materials Modification by Laser, Ion and Electron Beams, Chinese Ministry of Education, School of Physics and Optical Electronic Technology, Dalian University of Technology, Dalian 116024, China*
[2] *Institute of Plasma Physics, Chinese Academy of Sciences, PO Box 1126, Hefei 230031, China*
Corresponding author. E-mail: †*hding@dlut.edu.cn*
Received January 1, 2016; accepted May 25, 2016

Nuclear fusion has enormous potential to greatly affect global energy production. The next-generation tokamak ITER, which is aimed at demonstrating the feasibility of energy production from fusion on a commercial scale, is under construction. Wall erosion, material transport, and fuel retention are known factors that shorten the lifetime of ITER during tokamak operation and give rise to safety issues. These factors, which must be understood and solved early in the process of fusion reactor design and development, are among the most important concerns for the community of plasma–wall interaction researchers. To date, laser techniques are among the most promising methods that can solve these open ITER issues, and laser-induced breakdown spectroscopy (LIBS) is an ideal candidate for online monitoring of the walls of current and next-generation (such as ITER) fusion devices. LIBS is a widely used technique for various applications. It has been considered recently as a promising tool for analyzing plasma-facing components in fusion devices in situ. This article reviews the experiments that have been performed by many research groups to assess the feasibility of LIBS for this purpose.

Keywords LIBS, nuclear fusion, plasma-facing components

PACS numbers 42.62.Fi, 52.38.Mf

1 Introduction

During tokamak operation, plasma-facing components (PFCs) are subjected to harmful processes, including erosion, redeposition, and fuel retention, due to the severe interaction between edge plasmas and the inner walls of the fusion device chambers and divertors. Consequently, the PFCs are eroded and then redeposited in the form of layers on the surfaces, which can flake and produce dust. These phenomena can affect the overall system performance expected in ITER as well as in other fusion tokamaks and can also raise safety issues. Hence, the condition of first-wall materials should be properly monitored to ensure continuous and fault-free operation, and it is mandatory to study plasma–wall interaction (PWI) to avoid both damage to PFCs and pollution of the plasma [1–4].

Wall erosion, material transport, and fuel retention are known to be factors that shorten the lifetime of ITER and give rise to safety issues. These factors, which must be understood and solved early in the process of fusion reactor design and development, are among the most important concerns for the community of PWI researchers. The main wall diagnostic methods are offline methods and include nuclear reaction analysis [5], secondary ion mass spectrometry (SIMS) [6, 7], thermal desorption spectrometry [8, 9], X-ray photoelectron spectroscopy [10], Auger electron spectroscopy [11], and energy-dispersive X-ray spectroscopy [12]. Using these methods, Whyte *et al.* [13] measured the deuterium retention on the divertor tiles of the JET tokamak and found that the outer divertor strike point undergoes net erosion. Further, the inner divertor is a region of net redeposition, with deuterium codeposition rates of ~ 20 $\mu g \cdot m^2 \cdot s^{-1}$. Oya *et al.* [14] investigated the behavior of hydrogen and deuterium retained in the PFCs of the JT-60U tokamak and found that the behavior of hydrogen and deuterium and the chemical state of graphite were affected by the temperature of the surface, the position of the strike point, and the particle flux during operation.

*Special Topic: The 1st Asian Symposium on Laser-induced Breakdown Spectroscopy (Eds. Xiao-Yan Zeng, Zhe Wang & Yoshihiro Deguchi).

Rudakov *et al.* [15] studied the carbon erosion and redeposition and hydrogenic retention in the gaps between the PFCs of the DIII-D tokamak and confirmed that the hydrogenic retention in the PFC gaps was reduced at elevated temperature.

However, very few investigations of PFC diagnosis have been reported owing to the lack of in situ diagnostic methods for tokamaks. In situ experimental monitoring of compositional changes in the PFCs' surface layer can provide useful information on possible plasma pollution and fuel retention. In addition, models of the impurity deposition, erosion, or fuel retention need to be validated using experimental data. To this end, suitable diagnostic techniques that can perform depth profiling analysis of the superficial layers of the PFCs have been developed. Owing to the typical constraints of fusion devices, the measuring apparatus must be noninvasive, remote, and sensitive to light elements [1, 16]. Laser techniques are currently among the most promising methods that can solve these open ITER issues, and laser-induced breakdown spectroscopy (LIBS) is an ideal candidate for online monitoring of the walls of current and next-generation (such as ITER) fusion devices.

LIBS is a well-established tool for microdestructive characterization owing to its flexibility and ability to reach difficult-to-access structures and the possibility of installation on remotely controlled devices. It has been regarded as a future superstar for chemical analysis for years because of its unique features such as little or no sample preparation, remote sensing, and fast and multi-element analysis. In LIBS, vaporization and excitation are performed using a high-power focused laser pulse. Pulses from a laser are focused on the sample using a lens, and the plasma light is collected by a fiber optic cable coupled to a spectrometer. Each firing of the laser produces a single LIBS measurement. Over the past several years, LIBS has been applied to many studies on various subjects [17]. This paper reviews the reported results on the use of LIBS in nuclear fusion technology.

2 Effect of LIBS parameters on PFCs

Farid *et al.* [18] studied variations in the electron temperature and density as a function of the laser wavelength and irradiance. Laser ablation of tungsten was performed at 1064, 532, and 355 nm at atmospheric pressure to determine the suitability of LIBS for in situ diagnosis of PFCs. Stark broadening and Boltzmann plots were used to measure the electron density and temperature, respectively, of a laser-produced tungsten plasma. Figure 1 shows that at a constant laser irradiance (1.05×10^{15} W·m^{-2}), the maximum temperature (16 304 K) was reached at 1064 nm. The maximum electron density (1.12×10^{18} cm^{-3}) was observed at 355 nm. Variations in the electron temperature and density as a function of the laser irradiance and time were also discussed.

Farid *et al.* [19] investigated the effect of atmospheric conditions of Ar, N_2, and He at reduced pressure (2.0×10^{-4} – 5 mbar) on the physical processes of the atomic and background emission, mass ablation, electron density, and temperature of a laser-produced Mo plasma. This work adapted LIBS for in situ diagnosis and cleaning of the first mirrors. The obtained results strongly indicate that the pressure and physical properties of the background gases play a crucial role in interpreting the emission (line and continuum background) and characteristic parameters (electron density and temperature) of the plasma (Fig. 2). The plasma shielding effect was found to be less pronounced for a He environment, and it led to enhanced material evaporation from the target surface. This work could provide important reference

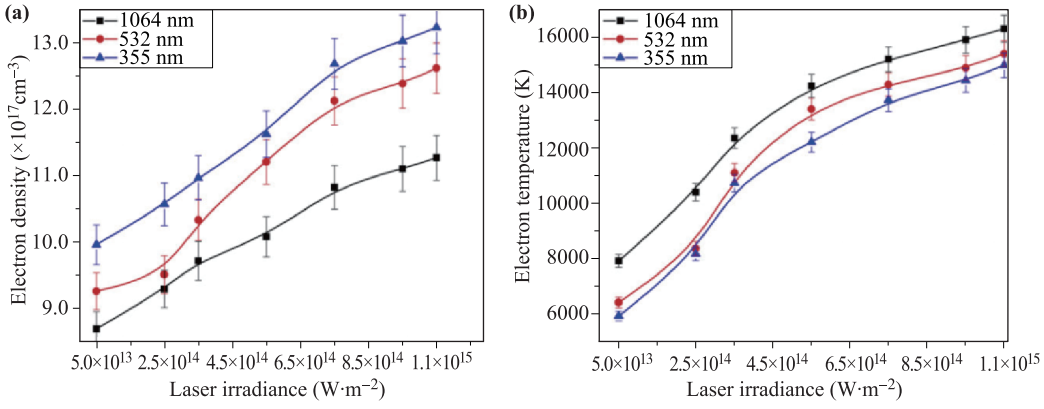

Fig. 1 Variations in **(a)** electron density and **(b)** temperature of laser-produced tungsten plasma under laser irradiance at wavelengths of 1064, 532, and 355 nm using a Nd:YAG laser [18].

data for the design and optimization of LIBS systems involved in PFC diagnostics.

Hai *et al.* [20] studied the effect of the magnetic field strength on LIBS at various pressures for the EAST tokamak. Aluminum (replaced Be)–lithium alloys were used as a substitute for a uniform lithium deposition layer on the first wall. Detailed information on the divertor tiles (multi-element-doped graphite) and aluminum–lithium alloys were obtained by analyzing the spectra from 200 to 980 nm. As shown in Fig. 3, under a magnetic field (0.94 T), the intensity of various line emissions obtained from the constituent materials of the samples were enhanced by >2 times owing to the increase in the effective plasma density and temperature resulting from magnetic confinement. The effect of the magnetic field on the emission intensity of LIBS at different pressures (1.0×10^{-5}–1000 mbar) would help us to develop a quantitative LIBS approach to monitor impurity deposition and fuel retention on the first wall.

Liu *et al.* [21] studied the variations in the atomic emission lines and laser-produced plasma plume as a function of the magnetic field. The results indicated that the LIBS intensity of the Al and Li emission lines is boosted as the magnetic strength increases. Typically, the intensity of the Al I and Li I spectral emission can be magnified by 1.5–3 times in a steady magnetic field of 1.1 T compared with that in the field-free case. In addition, in this investigation, time-resolved images of the laser-produced plume were recorded by employing a fast intensified charge-coupled device (ICCD) camera (Fig. 4). The results show that in the presence of a magnetic field, the luminance of the plasma is enhanced and the time of persistence is increased significantly, and the plasma plume splits into two lobes. The probable reason for the enhancement is the magnetic confinement effect, which increases the number density of excited atoms and the population of species in a high-energy state. In addition, the electron temperature and density are also augmented

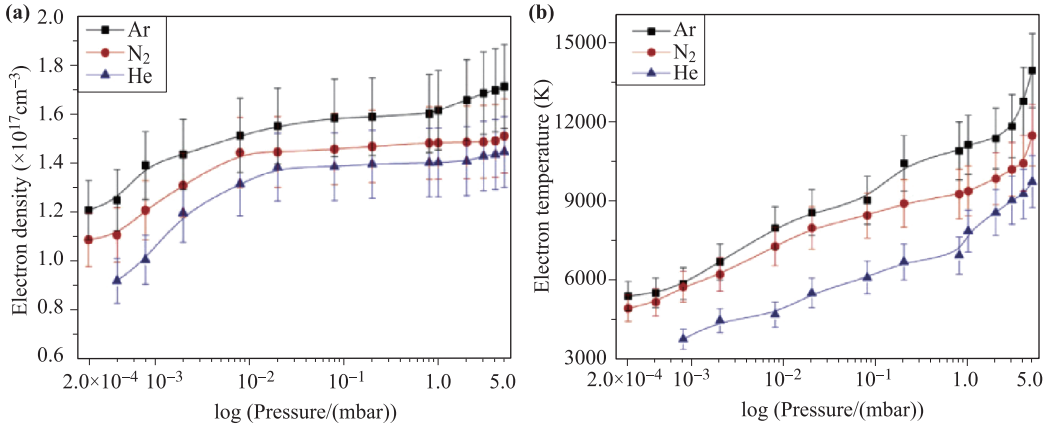

Fig. 2 Variations in **(a)** electron density and **(b)** temperature of laser-produced Mo plasma in Ar, N_2, and He environment at pressures ranging from 2.0×10^{-4} to 5 mbar [19].

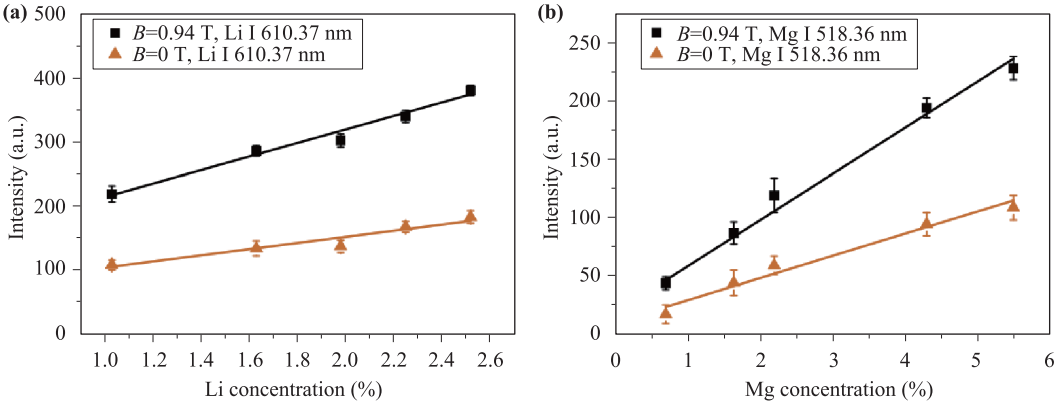

Fig. 3 Calibration curve of Li I (610.37 nm) and Mg I (518.36 nm) in the absence and presence of a magnetic field. LIBS spectra were recorded at a laser energy density of 15 J·cm^{-2} at 3×10^{-5} mbar [20].

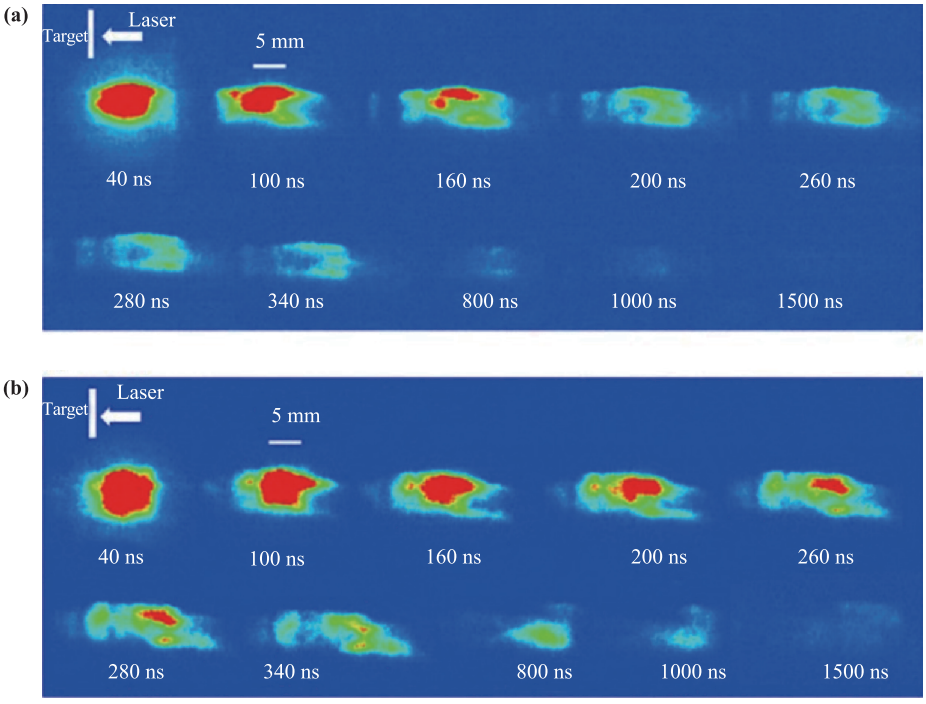

Fig. 4 Spectrally integrated and time-resolved images of nanosecond laser ablation of Al–Li alloy obtained using an ICCD camera with and without magnetic confinement. The applied gate time of the intensifier was 3 ns. **(a)** Without a magnetic field ($B = 0$ T), **(b)** with a magnetic field ($B = 1.1$ T) [21].

by the magnetic field compared to those in the field-free case.

3 Enhancement of LIBS sensitivity

Hai *et al.* [22] applied the collinear dual-pulse LIBS (DP-LIBS) configuration to overcome the sensitivity shortcomings of the conventional single-pulse LIBS (SP-LIBS) technique under vacuum. The plasma emission signal dependence on the interpulse delay at 3.5×10^{-3} Pa was systematically studied (Fig. 5), and the results were compared with those obtained using a single laser pulse with an energy corresponding to the sum of the two pulses. For a molybdenum tile, it was found that the atomic spectral lines of Mo were enhanced by a factor of 6.5 when an interpulse delay of 1.5 s was applied. For an exposed divertor tile, significant increases in the emission line intensities of various minor elements (such as Mo, Si, Fe, Cr, Ti, Ni, and Ca) were observed by DP-LIBS, whereas no spectral signal was obtained in SP-LIBS. This collinear DP-LIBS technique would help us to develop a more promising system to monitor fuel retention and impurity deposition on the PFCs of EAST.

Hai *et al.* [23] applied LIBS as an online control technique for the laser cleaning process of the polluted first mirror of the HL-2A tokamak. Spectroscopic study of the plasma emission can be used to determine the elemental composition of the ablated materials. The codeposition layer (approximately 0.8 lm) was completely removed after multiple pulses at 0.76 J·cm^{-2}, but the plasma initiated by the cleaning laser pulse was too weak to produce LIBS signals. Figure 6 shows that notable enhancement of the signal emission was observed using DP-LIBS. Real-time monitoring and accurate identification of the interface boundary can provide important information regarding the cleaned mirror surface in order to avoid undercleaning. Thus, DP-LIBS also has great potential for online measurement of laser ablation of the ultrathin codeposition layer on the first mirrors of the HL-2A tokamak during cleaning.

Zhao *et al.* [24] applied polarization-resolved LIBS (PR-LIBS) to reduce the background continuum and enhance the resolution and sensitivity of LIBS. Al (as a substitute for Be) and the first-wall materials tungsten and molybdenum were used to investigate the polarized continuum emission and signal-to-background ratio (SBR). A Nd:YAG laser with first, second, and third harmonics was used to produce plasma. The effects of the laser polarization plane, environmental pressure, and polarizer detection angle were investigated. The spectra obtained without using a polarizer (i.e., LIBS spectra) were

compared with those obtained using PR-LIBS (Fig. 7). The distribution of the emission spectral intensity was observed to follow Malus' law with respect to variation in the angle of detection of the polarizer. The spectra obtained by PR-LIBS had a higher SBR and greater stability than those obtained by LIBS, thus exhibiting enhanced reliability of LIBS for quantitative analyses. A comparison of the results for Al, Mo, and W showed that W exhibited a higher continuum with stronger polarization than the low-Z elements.

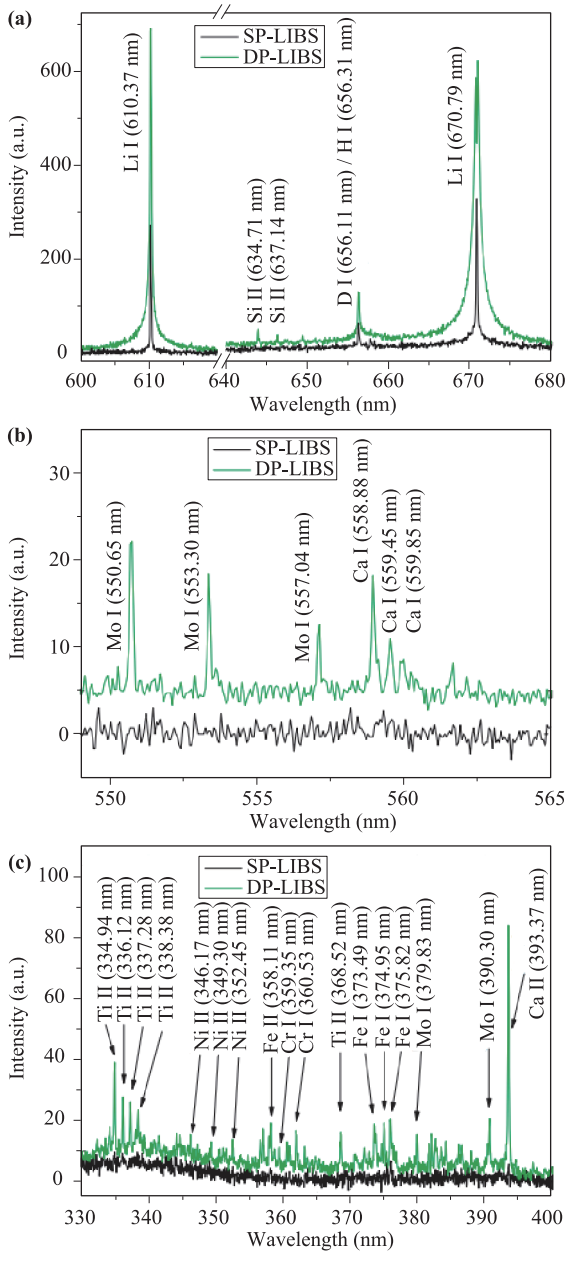

Fig. 5 Comparison of LIBS spectra obtained at 3.5×10^{-3} Pa for an exposed divertor tile (DM2-2012) in the range of **(a)** 600–680 nm, **(b)** 549–565 nm, and **(c)** 330–400 nm by SP-LIBS and DP-LIBS [22].

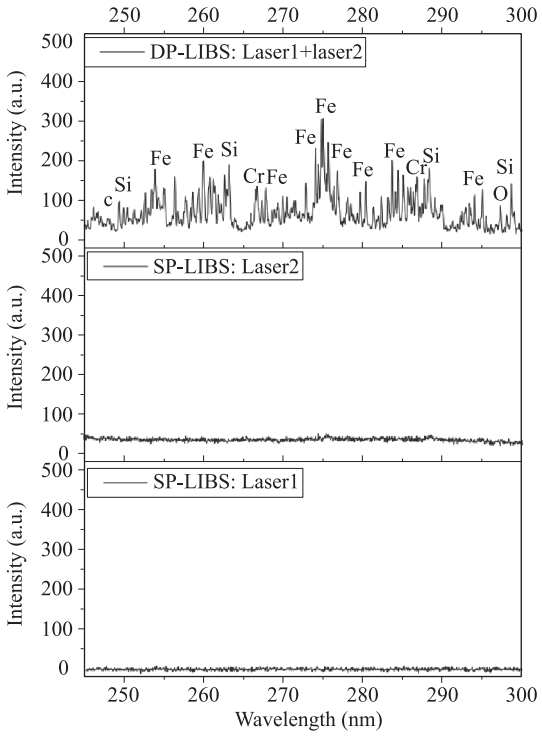

Fig. 6 Comparison of LIBS spectra obtained for the polluted mirror surface by single-pulse and double-pulse systems [23].

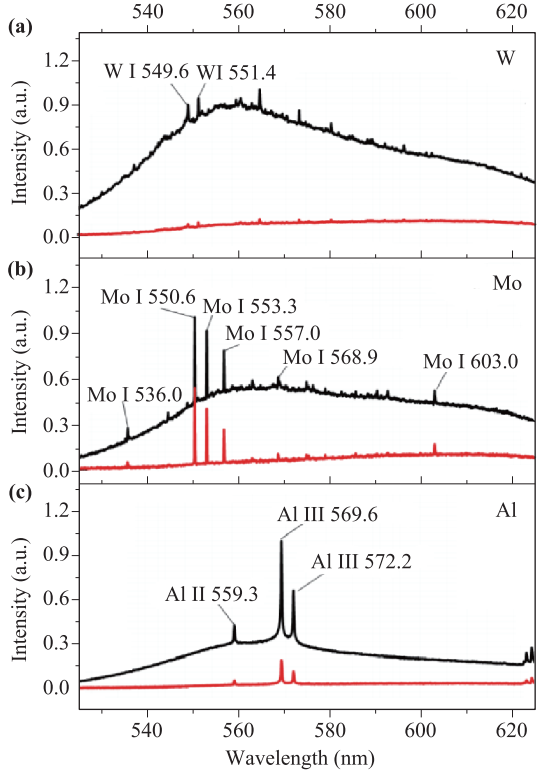

Fig. 7 Comparison of LIBS and PR-LIBS signals for **(a)** W, **(b)** Mo, and **(c)** Al. A linearly polarized laser beam (1064 nm) with a fluence of 30.57 J·cm^{-2} was used to produce the plasma [24].

Li *et al.* [25] studied the variations in the LIBS signal as a function of the spatial position using a LIBS system with spatially resolved collection. The spatial profiles of the LIBS signals of C, Si, Mo, and the continuous background were measured. Moreover, the effects of the laser spot size and laser energy density on the LIBS signals of C, Si, Mo, and H were also investigated. The results showed that the distribution of the C, Si, and Mo peaks' intensities first increased and then decreased from the center to the edge of the plasma plume. As shown in Fig. 8, there was a maximum value at $R \approx 1.5$ mm from the center of the plasma plume. This work aims to improve the understanding of ablating plasma dynamics in very low pressure environments and provide guidance for optimization of the LIBS system in the EAST device.

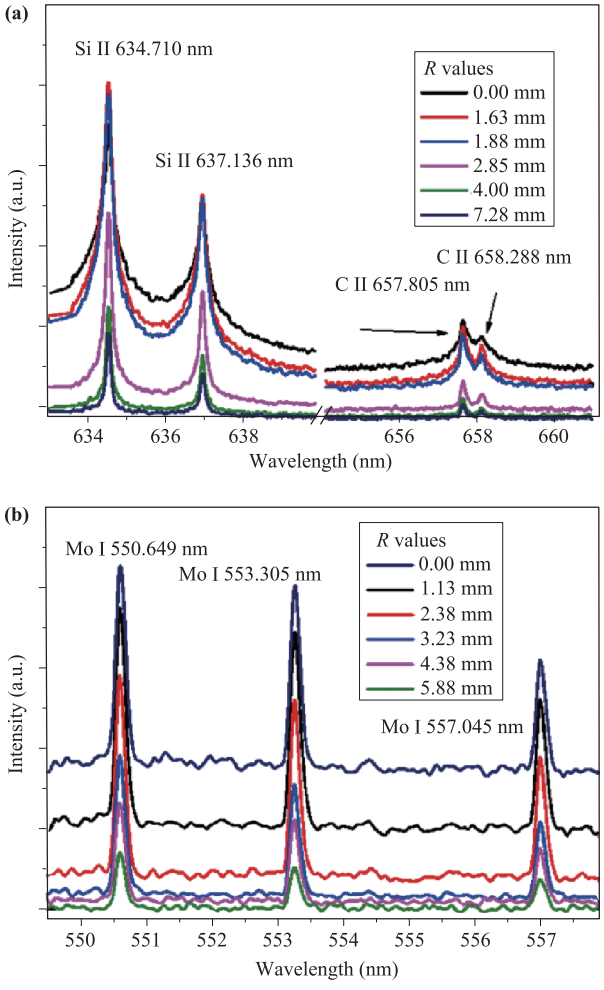

Fig. 8 LIBS spectra of **(a)** doped graphite and **(b)** titanium–zirconium–molybdenum at different spatial positions. At $R = 0$ mm, the fiber collected the emission signal from the center of the plasma plume. The laser energy density was 4.6 J·cm^{-2} [25].

4 LIBS of PFCs in the lab

LIBS has been applied to investigate ITER-like deposits under laboratory conditions to simulate a long working distance and to validate the accuracy and reproducibility of LIBS for future application in tokamaks.

Li *et al.* [26] studied the distribution of deuterium retention from a depth of 0.5 to 4 μm in the lithium–deuterium codeposition layer of EAST divertor tiles from the EAST 2012 campaign. The deuterium/hydrogen concentration ratio was estimated at 0.17 ± 0.02 in the lithium–deuterium codeposition layer (Fig. 9). Moreover, the depth profile behaviors of lithium and deuterium indicate that deuterium retention in the divertor tiles resulted from lithium–deuterium codeposition processes during deuterium discharge in EAST.

Hai *et al.* [27, 28] investigated the depth profiles of elements in divertor tiles. Detailed information on the compositions at superficial and deep positions in the first wall of divertor tiles can be obtained by analyzing the spectra from 200 to 980 nm. A decrease in the concentrations of the depositional elements, such as Li, was clearly observed at depths from 0 to 100 μm, but the concentrations of the substrate elements were found to be relatively uniform at these depths after dozens of laser pulses. The linear correlation approach was applied to improve the accuracy of the impurity depth profile and identify the interface boundary between the deposition layer and the substrate for the first time (Fig. 10). Maps characterizing the quasi-three-dimensional distribution of multiple elements in the impurities deposited in the gaps between divertor tiles were also obtained (Fig. 11).

These works would improve the understanding of the deuterium retention and lithium–deuterium codeposition mechanisms and provide guidance for optimization of the

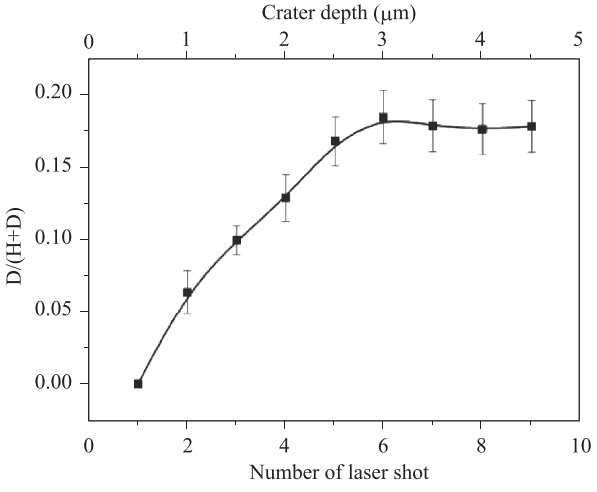

Fig. 9 Depth profile of the D/(H+D) concentration ratio as a function of the number of laser shots [26].

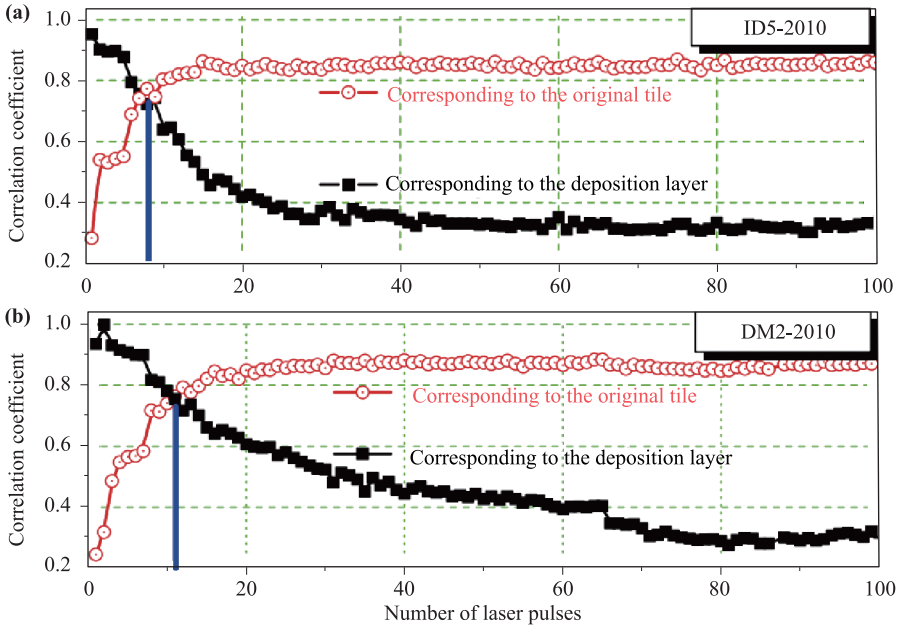

Fig. 10 Correlated depth profiles of the deposition layer surface and original tile surface. Vertical blue line indicates the location of the interface between the impurity deposition layer and the substrate [27].

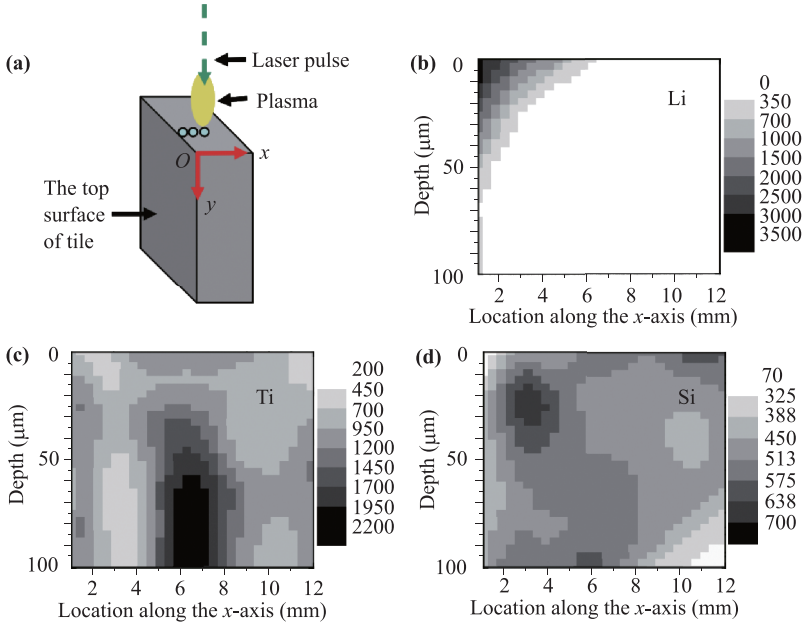

Fig. 11 **(a)** Schematic illustration of depth profile analysis on the side of the tile. Distribution of **(b)** Li, **(c)** Ti, and **(d)** Si on the sides of the divertor tiles. Depth is along the y axis. Gray scale images indicate the concentrations of the elements [28].

LIBS system, which will be a unique and useful diagnostic approach for EAST.

Mercadier *et al.* [29, 30] and Semerok *et al.* [31] performed a LIBS experiment on ITER-like materials. They applied an infrared laser a with 4 ns pulse duration to ablate hydrogen- and deuterium-containing carbon fiber composite (CFC) under argon at reduced pressure. The ablation depth was measured by microscopic analyses of the irradiated sample surface. According to the time-of-flight characteristics of the hydrogen and deuterium Balmer α spectral lines and the different atomic masses of both isotopes, hydrogen was found to expand slightly more quickly into the low pressure argon atmosphere than deuterium (Fig. 12). In addition, they explored the

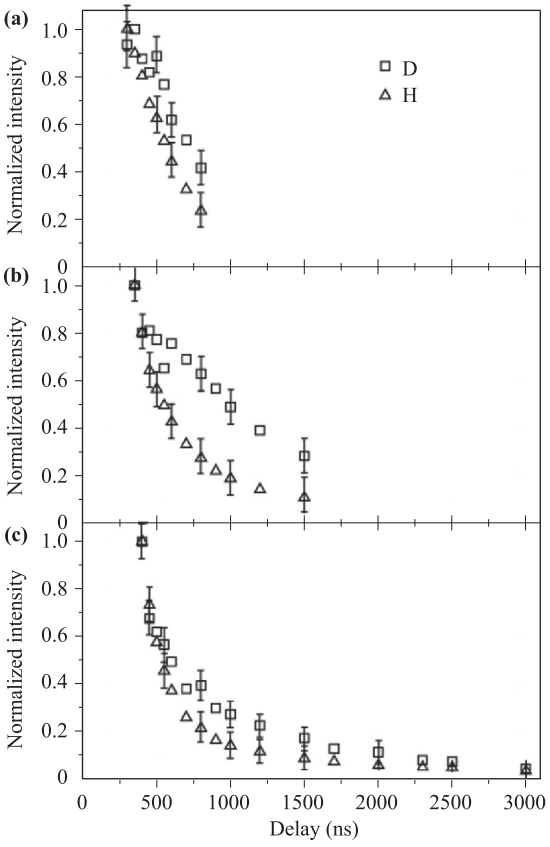

Fig. 12 Normalized intensities of Hα and Dα as functions of time recorded during ablation of CFC under argon atmosphere at **(a)** 1×10^2 Pa, **(b)** 2×10^2 Pa, and **(c)** 5×10^2 Pa. The observation distance was 1.5 mm, and the duration of the observation gate was set to 50 ns for (a) and 100 ns for (b) and (c) [29].

expansion dynamics of ionized and neutral species within the ablation plume and investigated the time evolution of the plume intensity and size. In particular, a parametric study including the laser fluence, pulse duration, and gas pressure was performed to determine the optimized operational conditions for LIBS analyses with samples from the Tore Supra reactor.

Almaviva *et al.* [32, 33] and Fantoni *et al.* [34] used LIBS to determine the atomic composition of multilayered samples simulating the tiles of PFCs in next-generation fusion machines such as ITER (Fig. 13). The effects of the time delay and laser fluence on the LIBS sensitivity at reduced pressure were examined to determine suitable operating conditions for analytical applications. Some atomic species in the superficial layer were analyzed quantitatively using a calibration-free LIBS approach in the time window in which local thermal equilibrium was assumed.

Huber *et al.* [35, 36] presented a feasibility study of LIBS for the development of an in situ diagnostic for the characterization of deposition layers on PFCs in fusion devices. LIBS would be preferentially applied in the presence of a toroidal magnetic field and under high-vacuum conditions. The impact of the laser energy densities on the laser-induced plasma parameters, and thus on the number of emitted photons and on the reproducibility of the LIBS method, was studied in laboratory experiments and in TEXTOR on fine-grained graphite (EK98) as well as on bulk W samples coated with carbon and metallic-containing deposits. The effect of magnetic fields and of ambient pressures ranging from 2×10^{-4} Pa to 10 Pa on the carbon plasma plume produced by the LIBS technique was studied in TEXTOR between plasma pulses (Fig. 14). The possibility of applying this method to ITER was discussed.

Karhunen *et al.* [37, 38] studied the inner divertor of the ITER-like wall of JET using LIBS to show the applicability of the method in JET and ITER. The elemental depth profiles agreed with those given by earlier SIMS measurements (Figs. 15 and 16). Deuterium was detected in the deposited layers and successfully distinguished from hydrogen. The results of these studies support LIBS as a promising in situ solution to replace the present post-mortem methods of monitoring metallic deposited layers.

The final purpose of using LIBS in ITER is to analyze the wall material quantitatively and thus measure the amount of fuel retention and deposition in and on the wall. However, simulation of LIBS is a cumbersome task because many nonlinear processes occur during LIBS. The mechanism of laser ablation is not yet known, and the vacuum boundary condition is still a challenging research topic in the fluid dynamics used in LIBS simulation in vacuum. In addition, many other problems such as heat conduction through the target and plasma formation, expansion, shielding, and emission must be considered. We have developed a professional package of codes called Dalian University of Technology Package for Laser Ablation and Plasma Simulation (DUT-LAPS) to handle these issues. DUT-LAPS was developed to simulate i) the laser ablation of target samples, ii) LIBS, iii) the dynamics of the plasma plume, and iv) damage to the tokomak wall due to plasma interaction [39].

Using DUT-LAPS, we developed a model and evaluated it experimentally for nanosecond laser ablation of W on the basis of the more likely phenomenon of explosive partial sublimation of a superheated irradiated zone and the resulting formation of a rarefaction wave that propagates through the vacuum. Many other aspects of LIBS simulation are under study according to this new model using DUT-LAPS. However, much elaboration by the LIBS community is required to obtain a very clear picture of LIBS mechanisms and the many complicated phenomena involved.

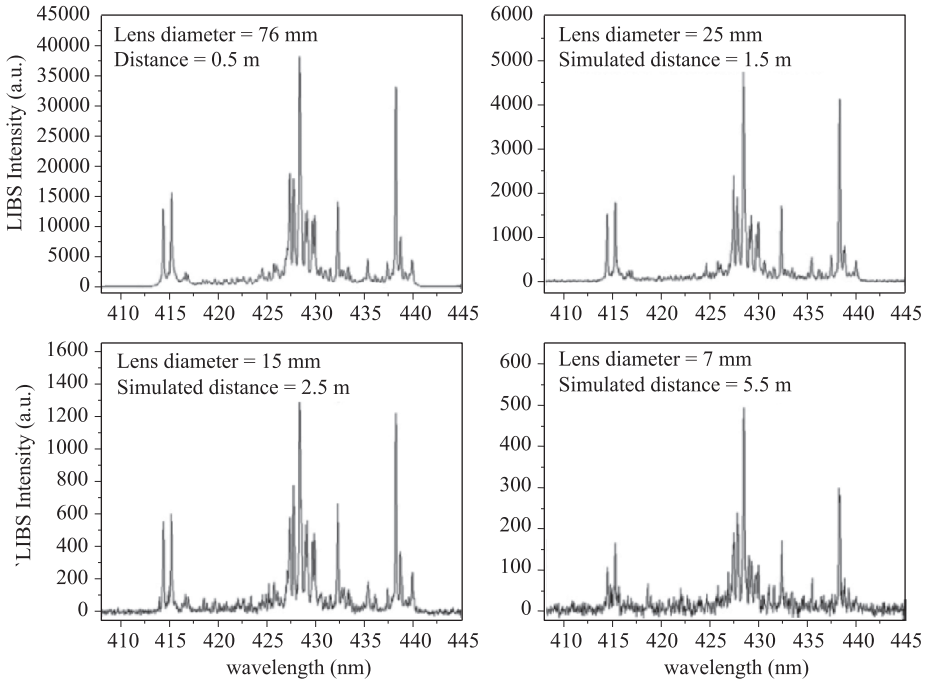

Fig. 13 Sequence of spectra from the titanium substrate, obtained by partially screening the collecting lens (note the different vertical scales) [33].

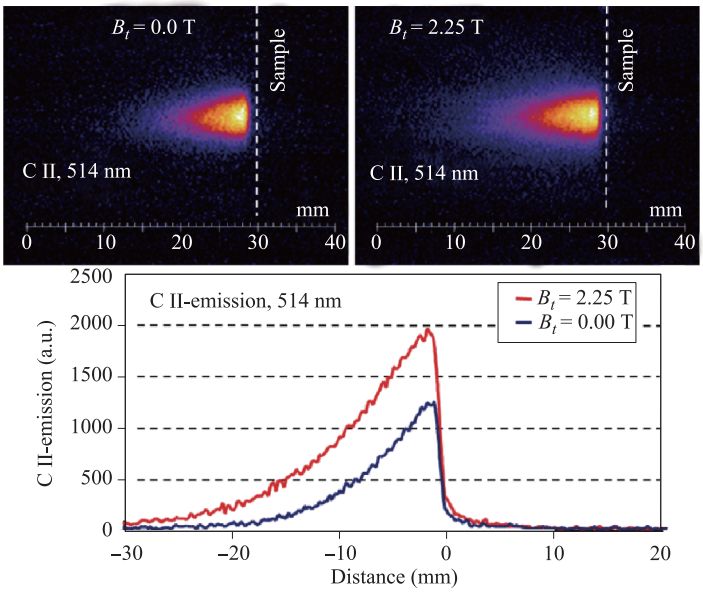

Fig. 14 Effect of a magnetic field on the laser-induced plasma plume in TEXTOR [35].

5 LIBS study of linear plasma generators

The Magnum-PSI device is the largest linear plasma simulator for plasma surface interaction at the FOM Institute DIFFER. This device was built to reproduce the plasma conditions expected in the divertor of future fusion devices, both in the steady state and during transient events, such as edge localized modes (ELMs) [40, 41]. Li *et al.* [42] developed an in situ LIBS system for analysis of samples immediately after plasma exposure in the target exchange chamber of Magnum-PSI. Elemental depth profiles can be extracted from the measurements. Deuterium retention inside both pure and lithiated tungsten was investigated in Magnum-PSI by in situ LIBS. After deuterium plasma exposure, deuterium

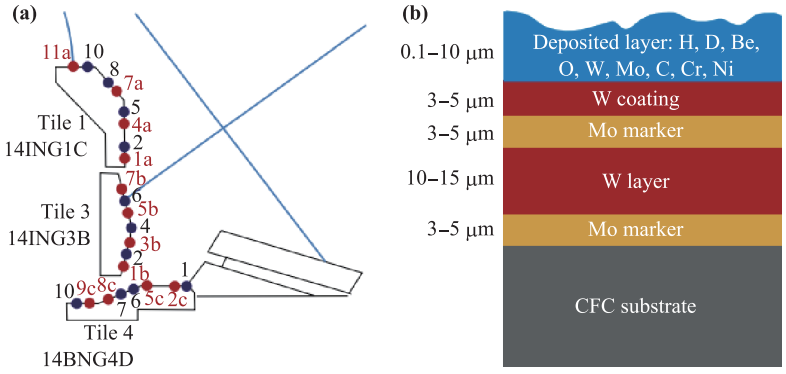

Fig. 15 **(a)** Locations of the samples selected for LIBS (*red*) and SIMS (*blue*) studies in the inner divertor of JET; **(b)** layered structure of the studied samples [37].

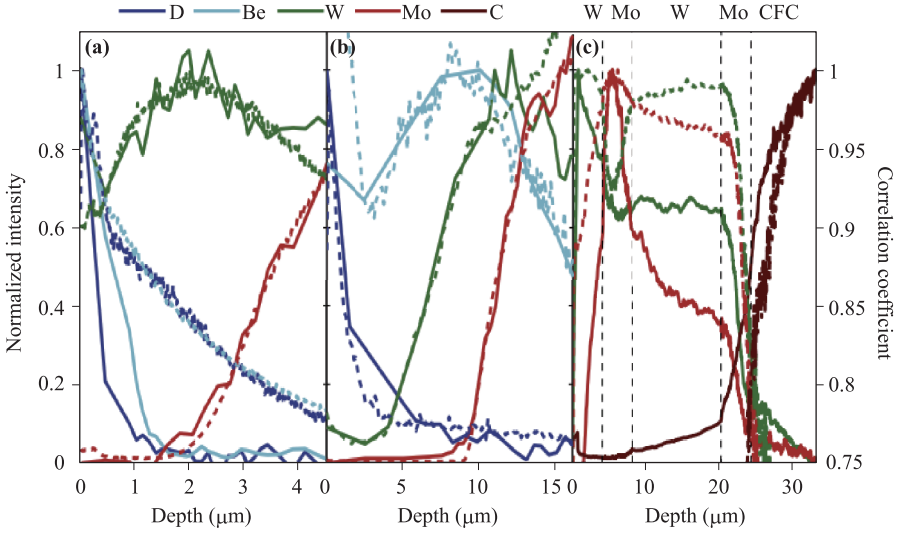

Fig. 16 Elemental depth profiles detected for samples **(a)** 1a (LIBS, *solid line*) and 2 (SIMS, dashed line) and **(b)** 11a (LIBS, *solid line*) and 10 (SIMS, *dashed line*) on Tile 1; **(c)** layered structure of sample 5c on Tile 4 measured by LIBS at a fluence of 5 J·cm^{-2}. Solid profiles are determined directly from the normalized line intensities; dashed profiles represent the correlation coefficients (right y axis) between spectra from different layers [37].

retention could be saturated in the lithiation layer, and the lithium in the lithiated layer is chemically bound with deuterium (Fig. 17). As the D fluence increases from 1.9×10^{25} to 6.2×10^{25} m^{-2}, the D retention was saturated for both the pure and lithiated W samples. Moreover, the Li intensities decreased after D plasma exposure and then remained stable owing to the balance between Li erosion and redeposition. The D and H signals of lithiated W are significantly more intense than those of pure W.

Piip *et al.* [43] and Paris *et al.* [44] studied the elemental depth profiles of tungsten-coated samples and diamond-like carbon samples that were exposed to Magnum-PSI or Pilot-PSI plasma using the steady-state and ELM-like regimes (Fig. 18). These results can be valuable for the application of LIBS as a diagnostic technique for PFCs in fusion reactors.

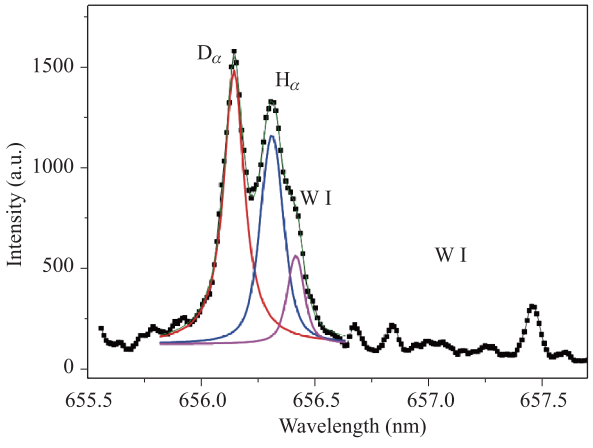

Fig. 17 LIBS spectrum of lithiated W after D plasma exposure (D fluence, 6.2×10^{25} m^{-2}) [42].

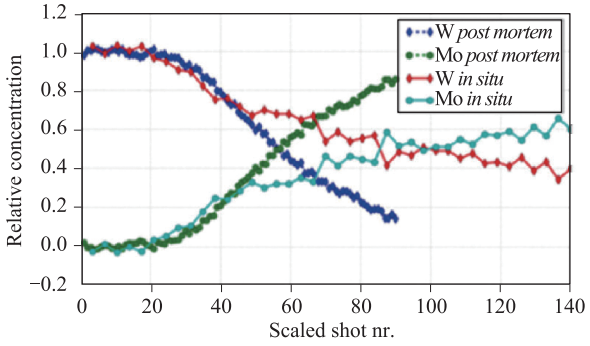

Fig. 18 *In situ* and post-mortem LIBS elemental depth profiles of samples [43].

Li *et al.* [45] developed an in situ LIBS diagnostic system in a cascaded-arc plasma simulator called DUT-PSI to chemically image the three-dimensional distribution of lithium and impurities on the surface of the lithiated tungsten codeposition layer. The results indicate that lithium has a strong ability to draw hydrogen and oxygen (Fig. 19). The impurity components from the codeposition processes exhibit greater intensity on the surface of the codeposition layer. This work improves the understanding of the tungsten lithiation mechanism and is useful for applying LIBS as a wall-diagnostic technique for EAST.

6 LIBS experiments in tokamaks

A number of investigations in which the EAST divertor tiles and first wall were characterized using LIBS have been performed in the laboratory since the 2012 experimental campaign. The results indicated that the fuel (D) retention and impurity codeposition can be measured using LIBS at depths from 0.1 to 500 μm in the deposited layer. In the current investigation, an in situ LIBS system was installed in EAST in the 2014 experimental campaign (Fig. 20). The LIBS system consists of a pulsed Q-switched Nd:YAG laser (Brilliant Eazy, Quantel) and a LIBS2500+spectrometer (Ocean Optics Inc., U.S.). The laser was operated at a wavelength of 1064 nm with a 5 ns pulse width at a repetition rate of 10 Hz and power of 180 mJ/pulse. The laser beam was focused on the wall surface on the high-magnetic-field side with a laser power density of 2×10^{12} W·m^{-2} to generate plasma via a 3.0 m focal length quartz lens mounted at the H port of the EAST device. The ablated plasma light emission was collected in a direction nearly perpendicular to the target surface by a telescope optical system and guided into an optical fiber bundle coupled to the spectrometer, which has seven linear silicon CCD array detectors. This made it possible to analyze the LIBS emission at wavelengths of 200 to 920 nm at a spectral resolution of 0.06 nm using a single laser pulse. A few small ($10\times10\times3$ mm^3) marked tiles made of Mo, W, Mo+W, C+Mo, C+W, and La+W materials were mounted on the wall surface on the high-field side for LIBS analysis. The overview LIBS spectra of the marked tiles after exposure for a total of 47 441 shots as well as the Li wall conditioning are plotted in Fig. 21. The spectral signals of multiple elements (D, H, Li, Mo, W, Ti, La, Fe, and Si) were observed in situ using LIBS. In addition to the signals from the substrate materials of Mo, W, C, and La, the observed signals of D and H came from the fuel (H was used for isotope ex-

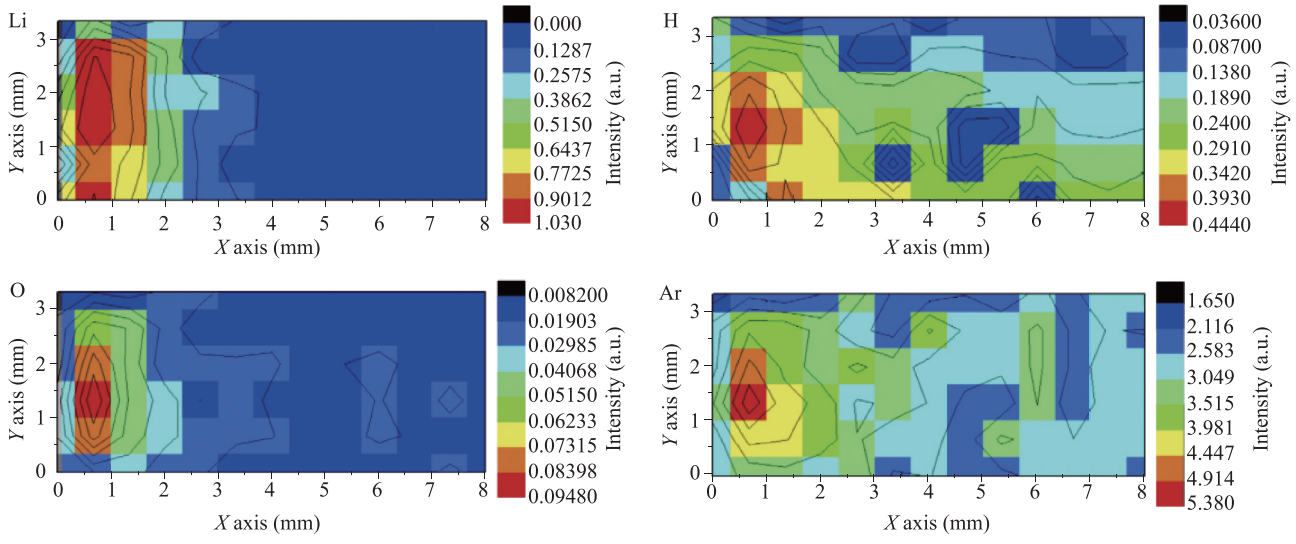

Fig. 19 Chemical imaging of two-dimensional distribution of elements on the surface of lithiated W with first laser shot [45].

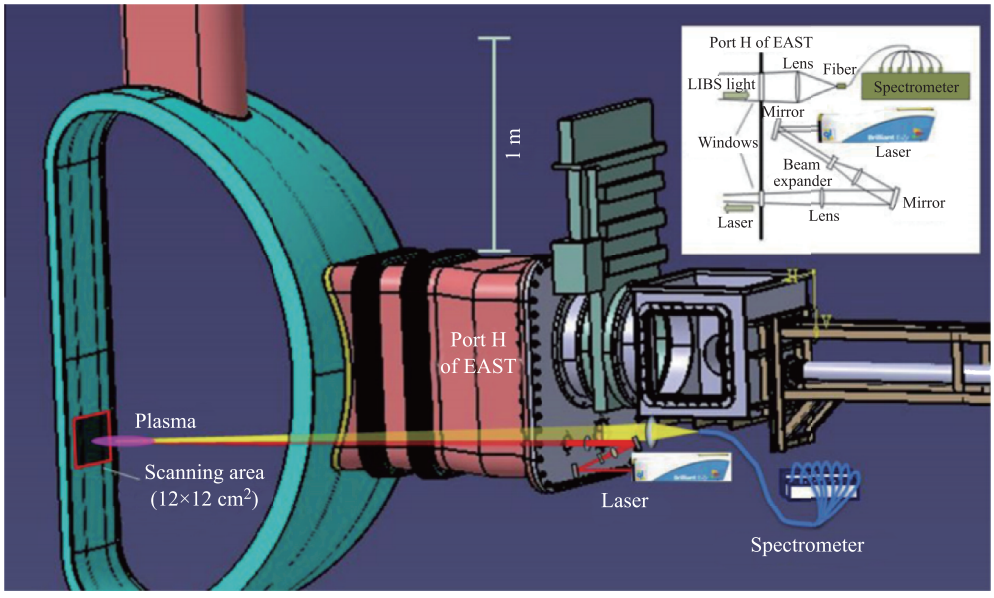

Fig. 20 Schematic of *in situ* LIBS system in EAST [26].

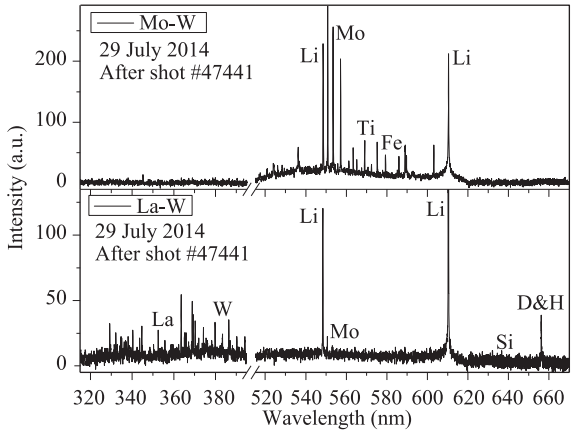

Fig. 21 LIBS spectra of Mo–W tile and La–W tile in first wall measured after shot #47441 of EAST discharge.

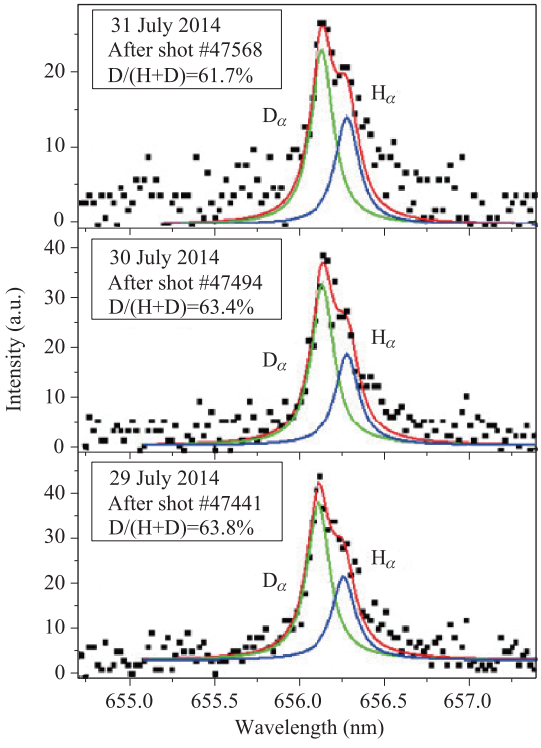

Fig. 22 Spectral signals of Dα and Hα in Li/D codeposition layer after various shot numbers of EAST discharge.

change experiments), and the Li signal was caused by Li wall conditioning. The other peaks of Ti, Fe, and Si were due to impurities deposited in the Li codeposition layer. During long-pulse operation of high-confinement plasma in EAST, Li wall conditioning could play an important role because Li conditioning would effectively remove H impurities from the gas phase and reduce H recycling by the Li/H codeposition processes. The LIBS signals of H and D in the deposited layer are shown in Fig. 22. On the basis of Fig. 22, the H/H+D ratio in the deposited layer was estimated as 34%–38%, which is much higher than the value (<5%) in the plasma phase. This indicates that Li/H codeposition can significantly reduce the H/H+D ratio in the plasma phase and enhance long-pulse H-mode plasma operation. Figure 23 shows the depth profiles of the deposited Li and the first wall material (Mo) in EAST calculated using the LIBS spectra. These profiles indicate that the thickness of the Li layer increases with EAST operation time but not lin-

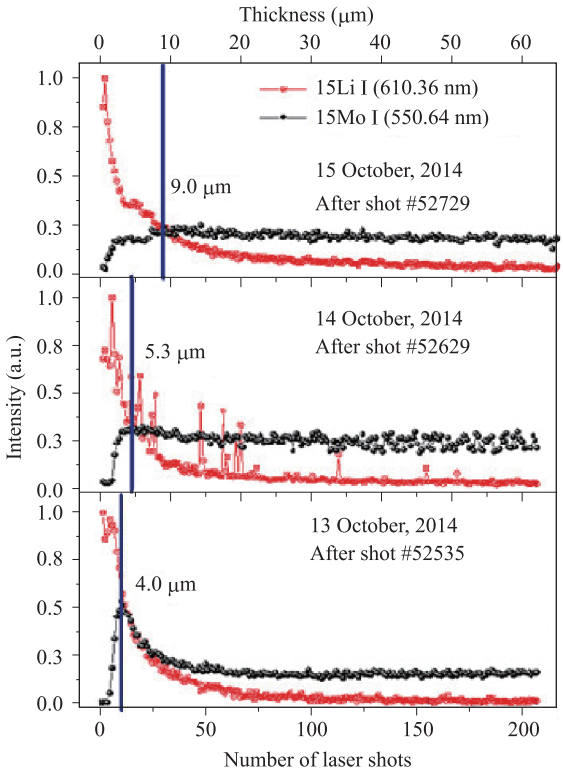

Fig. 23 Depth profiles of Li and the Mo tile. Vertical lines indicate the location of the interface between the deposited Li layer and the tile material (Mo).

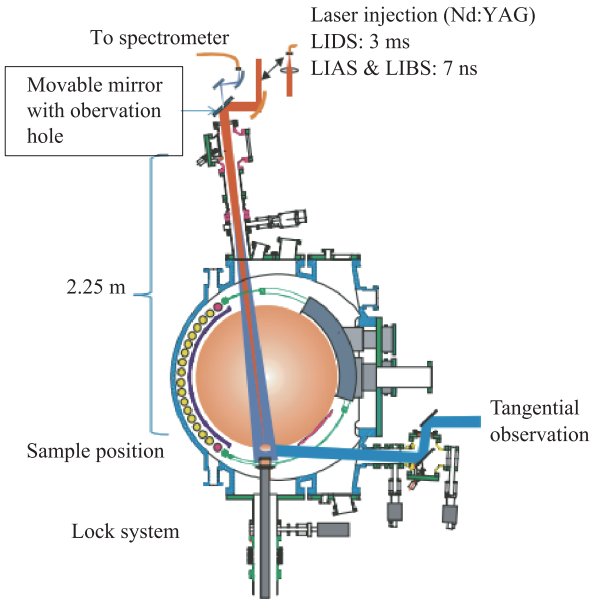

Fig. 24 Experimental set-up of laser-induced desorption spectroscopy (LIDS), laser-induced ablation spectroscopy (LIAS), and LIBS in TEXTOR [1].

early because the Li wall conditioning processes differed from day to day, and the layer would be removed by the main plasma of EAST as well as ion cyclotron resonance frequency discharge cleaning. In summary, an in situ LIBS diagnostic approach was established for the first time in EAST. The preliminary results demonstrate the potential of LIBS for in situ characterization of D/H retention and Li codeposition on the wall of EAST.

Experiments were conducted in the TEXTOR tokamak under neutral pressures of $<10^{-5}$ mbar on fine-grained pure graphite (EK98) (Fig. 24). Carbon was a candidate material for the first wall material of ITER and is still being used in some fusion devices such as DIII-D. A Nd:YAG laser expanded by a telescope system was guided into TEXTOR by means of six dichroic mirrors and was focused by a lens with a focal length of 2.5 m placed before the TEXTOR vacuum window. The samples were mounted on a rotatable probe holder that was introduced from the bottom of the device through a limiter lock system. The spot area determined by post-mortem surface analysis was 12.6 mm^2. The laser energy in front of the TEXTOR window was 1 J, and about 92% of the energy could reach the sample. A visible range (365–715 nm) spectrometer with high resolution (k/Dk = 20 000) was employed at the side to detect the emission spectra over an observation region 1.3 cm in diameter. A CCD camera with a time window of 20 ms was also employed to monitor the LIB emissions. As shown in Fig. 25, the LIBS signals were recorded and analyzed as the TEXTOR toroidal magnetic field was ramped from 0 to 2.25 T with 21 laser pulses in every TEXTOR shot before the plasma discharge was ignited. The first two shots were before the magnetic field ramp ($B = 0$ T), and the last one was in the flattop phase of the magnetic field ($B = 2.25$ or 2.4 T). The experiments were repeated in several TEXTOR shots [1, 46].

7 Conclusion

LIBS can be developed to measure and monitor the composition evolution of PFCs in EAST under laboratory conditions. To date, several aspects have been tested and explored by various groups. The main emphasis has been on the effect of the laser parameters and vacuum condition, the effect of the magnetic field, and the method used to enhance the LIBS sensitivity. A LIBS system has been developed for in situ characterization of the first wall in EAST since the 2014 experimental campaigns. These results can be valuable for the application of LIBS as an important diagnostic technique for the PFCs of next-generation fusion reactors.

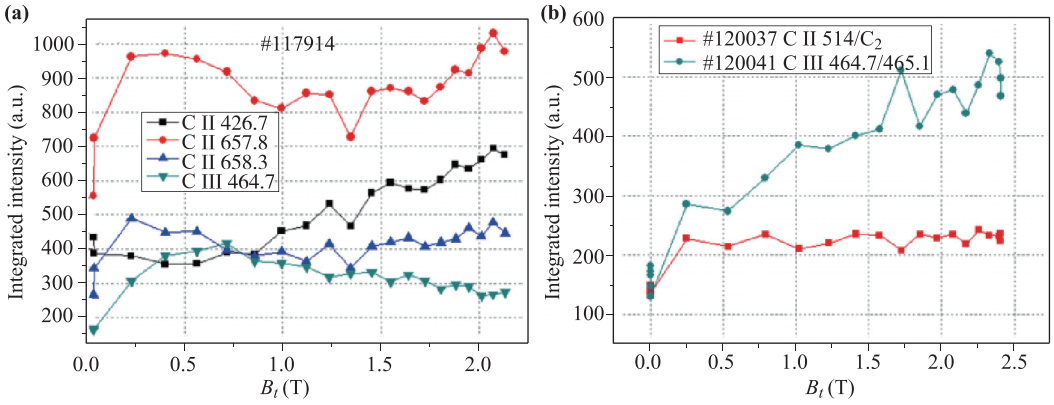

Fig. 25 Evolution of carbon lines produced by laser ablation of graphite in TEXTOR with magnetic field: **(a)** integrated intensity from spectra and **(b)** integrated intensity of CII and CIII from CCD images [46].

Acknowledgements This work was supported by the National Magnetic Confinement Fusion Science Program of China (Grant No. 2013GB109005), the National Science Foundation of China (Grant Nos. 11175035 and 11475039), the Chinesisch-Deutsches Forschungs Project (GZ768), the China Postdoctoral Science Foundation (Grant No. 2016M591423), and Fundamental Research Funds for the Central Universities (Grant Nos. DUT15RC(3)072, DUT15TD44, and DUT16TD13).

References

1. V. Philipps, A. Malaquias, A. Hakola, J. Karhunen, G. Maddaluno, S. Almaviva, L. Caneve, F. Colao, E. Fortuna, P. Gasior, M. Kubkowska, A. Czarnecka, M. Laan, A. Lissovski, P. Paris, H. J. van der Meiden, P. Petersson, M. Rubel, A. Huber, M. Zlobinski, B. Schweer, N. Gierse, Q. Xiao, and G. Sergienko, Development of laser-based techniques for *in situ* characterization of the first wall in ITER and future fusion devices, *Nucl. Fusion* 53(9), 093002 (2013)
2. G. Federici, C. H. Skinner, J. N. Brooks, J. P. Coad, C. Grisolia, A. A. Haasz, A. Hassanein, V. Philipps, C. S. Pitcher, J. Roth, W. R. Wampler, and D. G. Whyte, Plasma-material interactions in current tokamaks and their implications for next step fusion reactors, *Nucl. Fusion* 41(12), 1967 (2001)
3. G. Federici, P. Andrew, P. Barabaschi, J. Brooks, R. Doerner, A. Geier, A. Herrmann, G. Janeschitz, K. Krieger, A. Kukushkin, A. Loarte, R. Neu, G. Saibene, M. Shimada, G. Strohmayer, and M. Sugihara, Key ITER plasma edge and plasma–material interaction issues, *J. Nucl. Mater.* 313–316, 11 (2003)
4. M. Rubel, P. Wienhold, and D. Hildebrandt, Fuel accumulation in co-deposited layers on plasma facing components, *J. Nucl. Mater.* 290–293, 473 (2001)
5. K. Sugiyama, T. Hayashi, K. Krieger, M. Mayer, K. Masaki, N. Miya, and T. Tanabe, Ion beam analysis of H and D retention in the near surface layers of JT-60U plasma facing wall tiles, *J. Nucl. Mater.* 363–365, 949 (2007)
6. M. Mayer, V. Rohde, J. Likonen, E. Vainonen-Ahlgren, K. Krieger, X. Gong, and J. Chen, Carbon erosion and deposition on the ASDEX Upgrade divertor tiles, *J. Nucl. Mater.* 337–339, 119 (2005)
7. A. Yoshikawa, Y. Hirohata, Y. Oya, T. Shibahara, M. Oyaidzu, T. Arai, Y. Gotoh, K. Masaki, N. Miya, K. Okuno, and T. Tanabe, Hydrogen retention and depth profile in divertor tiles of Jt-60 exposed to hydrogen discharges, *Fusion Eng. Des.* 81(1–7), 289 (2006)
8. T. Shibahara, T. Tanabe, Y. Hirohata, Y. Oya, M. Oyaidzu, A. Yoshikawa, Y. Onishi, T. Arai, K. Masaki, K. Okuno, and N. Miya, Hydrogen retention of JT-60 open divertor tiles exposed to HH discharges, *Nucl. Fusion* 46(10), 841 (2006)
9. K. Katayama, T. Takeishi, Y. Manabe, H. Nagase, M. Nishikawa, and N. Miya, Tritium release behavior from the graphite tiles used at the dome unit of the W-shaped divertor region in JT-60U, *J. Nucl. Mater.* 340(1), 83 (2005)
10. T. Hino, K. Iwamoto, Y. Hirohata, T. Yamashina, A. Sagara, N. Noda, N. Inoue, Y. Kubota, N. Natsir, O. Motojima, T. Matsuda, T. Sogabe, K. Kuroda, and M. Yabe, Properties of boron coatings used as plasma facing material of fusion device, *Thin Solid Films* 253(1–2), 518 (1994)
11. E. Taglauer and G. Staudenmaier, Surface analysis in fusion devices, *J. Vac. Sci. Technol. A* 5(4), 1352 (1987)
12. J. Goldstein, D. E. Newbury, D. C. Joy, C. E. Lyman, P. Echlin, E. Lifshin, L. Sawyer, and J. R. Michael, Scanning Electron Microscopy and X-ray Microanalysis, 3rd Ed., New York: Springer, 2003
13. D. G. Whyte, J. P. Coad, P. Franzen, and H. Maier, Similarities in divertor erosion/redeposition and deuterium retention patterns between the tokamaks ASDEX Upgrade, DIII-D and JET, *Nucl. Fusion* 39(8), 1025 (1999)

14. Y. Oya, Y. Hirohata, Y. Morimoto, H. Yoshida, H. Kodama, K. Kizu, J. Yagyu, Y. Gotoh, K. Masaki, K. Okuno, T. Tanabe, N. Miya, T. Hino, and S. Tanaka, Hydrogen isotope behavior in in-vessel components used for DD plasma operation of JT-60U by SIMS and XPS technique, *J. Nucl. Mater.* 313–316, 209 (2003)
15. D. L. Rudakov, C. P. C. Wong, A. Litnovsky, W. R. Wampler, J. A. Boedo, N. H. Brooks, M. E. Fenstermacher, M. Groth, E. M. Hollmann, W. Jacob, S. I. Krasheninnikov, K. Krieger, C. J. Lasnier, A. W. Leonard, A. G. McLean, M. Marot, R. A. Moyer, T. W. Petrie, V. Philipps, R. D. Smirnov, P. C. Stangeby, J. G. Watkins, W. P. West, and J. H. Yu, Overview of the recent DiMES and MiMES experiments in DIII-D, *Phys. Scr.* T138, 014007 (2009)
16. A. Huber, B. Schweer, V. Philipps, N. Gierse, M. Zlobinski, S. Brezinsek, W. Biel, V. Kotov, R. Leyte-Gonzales, Ph. Mertens, and U. Samm, Development of laser-based diagnostics for surface characterisation of wall components in fusion devices, *Fusion Eng. Des.* 86(6–8), 1336 (2011)
17. Z. Wang, T. B. Yuan, Z. Y. Hou, W. D. Zhou, J. D. Lu, H. B. Ding, and X. Y. Zeng, Laser-induced breakdown spectroscopy in China, *Front. Phys.* 9(4), 419 (2014)
18. N. Farid, C. Li, H. Wang, and H. Ding, Laser-induced breakdown spectroscopic characterization of tungsten plasma using the first, second, and third harmonics of an Nd:YAG laser, *J. Nucl. Mater.* 433(1–3), 80 (2013)
19. N. Farid, H. Wang, C. Li, X. Wu, H. Y. Oderji, H. Ding, and G. N. Luo, Effect of background gases at reduced pressures on the laser treated surface morphology, spectral emission and characteristics parameters of laser produced Mo plasmas, *J. Nucl. Mater.* 438(1–3), 183 (2013)
20. R. Hai, P. Liu, D. Wu, Q. Xiao, L. Sun, and H. Ding, Effect of steady magnetic field on laser-induced breakdown spectroscopic characterization of EAST-like wall materials, *J. Nucl. Mater.* 463, 927 (2015)
21. P. Liu, R. Hai, D. Wu, Q. Xiao, L. Sun, and H. Ding, The enhanced effect of optical emission from laser induced breakdown spectroscopy of an Al-Li alloy in the presence of magnetic field confinement, *Plasma Sci. Technol.* 17(8), 687 (2015)
22. R. Hai, P. Liu, D. Wu, H. Ding, J. Wu, and G. N. Luo, Collinear double-pulse laser-induced breakdown spectroscopy as an in-situ diagnostic tool for wall composition in fusion devices, *Fusion Eng. Des.* 89(9–10), 2435 (2014)
23. R. Hai, X. Wu, Y. Xin, P. Liu, D. Wu, H. Ding, Y. Zhou, L. Cai, and L. Yan, Use of dual-pulse laser-induced breakdown spectroscopy for characterization of the laser cleaning of a first mirror exposed in HL-2A, *J. Nucl. Mater.* 447(1–3), 9 (2014)
24. D. Zhao, N. Farid, R. Hai, D. Wu, and H. Ding, Diagnostics of first wall materials in a magnetically confined fusion device by polarization-resolved laser-induced breakdown spectroscopy, *Plasma Sci. Technol.* 16(2), 149 (2014)
25. C. Li, D. Zhao, X. Wu, and H. Ding, Spatial resolution measurements of C, Si and Mo using LIBS for diagnostics of plasma facing materials in a fusion device, *Plasma Sci. Technol.* 17(8), 638 (2015)
26. C. Li, D. Zhao, Z. Hu, X. Wu, G. N. Luo, J. Hu, and H. Ding, Characterization of deuterium retention and co-deposition of fuel with lithium on the divertor tile of EAST using laser induced breakdown spectroscopy, *J. Nucl. Mater.* 463, 915 (2015)
27. R. Hai, N. Farid, D. Y. Zhao, L. Zhang, J. H. Liu, H. B. Ding, J. Wu, and G. N. Luo, Laser-induced breakdown spectroscopic characterization of impurity deposition on the first wall of a magnetic confined fusion device: Experimental Advanced Superconducting Tokamak, *Spectrochim. Acta B* 87, 147 (2013)
28. R. Hai, C. Li, H. B. Wang, H. B. Ding, H. S. Zhuo, J. Wu, and G. N. Luo, Characterization of Li deposition on the first wall of EAST using laser-induced breakdown spectroscopy, *J. Nucl. Mater.* 438, S1168 (2013)
29. L. Mercadier, J. Hermann, C. Grisolia, and A. Semerok, Plume segregation observed in hydrogen and deuterium containing plasmas produced by laser ablation of carbon fiber tiles from a fusion reactor, *Spectrochim. Acta B* 65(8), 715 (2010)
30. L. Mercadier, J. Hermann, C. Grisolia, and A. Semerok, Analysis of deposited layers on plasma facing components by laser-induced breakdown spectroscopy: Towards ITER tritium inventory diagnostics, *J. Nucl. Mater.* 415(1), S1187 (2011)
31. A. Semerok and C. Grisolia, LIBS for tokamak plasma facing components characterisation: Perspectives on in situ tritium cartography, *Nucl. Instrum. Methods Phys. Res. A* 720, 31 (2013)
32. S. Almaviva, L. Caneve, F. Colao, R. Fantoni, and G. Maddaluno, Laboratory feasibility study of fusion vessel inner wall chemical analysis by Laser Induced Breakdown Spectroscopy, *Chem. Phys.* 398, 228 (2012)
33. S. Almaviva, L. Caneve, F. Colao, R. Fantoni, and G. Maddaluno, Remote-LIBS characterization of ITER-like plasma facing materials, *J. Nucl. Mater.* 421(1–3), 73 (2012)
34. R. Fantoni, S. Almaviva, L. Caneve, F. Colao, A. M. Popov, and G. Maddaluno, Development of Calibration-Free Laser-Induced-Breakdown-Spectroscopy based techniques for deposited layers diagnostics on ITER-like tiles, *Spectrochim. Acta B* 87, 153 (2013)
35. A. Huber, B. Schweer, V. Philipps, R. Leyte-Gonzales, N. Gierse, M. Zlobinski, S. Brezinsek, V. Kotov, P. Mertens, U. Samm, and G. Sergienko, Study of the feasibility of applying laser-induced breakdown spectroscopy for *in-situ* characterization of deposited layers in fusion devices, *Phys. Scr.* T145, 014028 (2011)
36. N. Gierse, B. Schweer, A. Huber, O. Karger, V. Philipps, U. Samm, and G. Sergienko, In situ characterisation of

hydrocarbon layers in TEXTOR by laser induced ablation and laser induced breakdown spectroscopy, *J. Nucl. Mater.* 415(1), S1195 (2011)

37. J. Karhunen, A. Hakola, J. Likonen, A. Lissovski, M. Laan, and P. Paris, Applicability of LIBS for in situ monitoring of deposition and retention on the ITER-like wall of JET – Comparison to SIMS, *J. Nucl. Mater.* 463, 931 (2015)
38. J. Karhunen, A. Hakola, J. Likonen, A. Lissovski, P. Paris, M. Laan, K. Piip, C. Porosnicu, C. P. Lungu, and K. Sugiyama, Development of laser-induced breakdown spectroscopy for analyzing deposited layers in ITER, *Phys. Scr.* T159, 014067 (2014)
39. H. Y. Oderji, N. Farid, L. Sun, C. Fu, and H. Ding, Evaluation of explosive sublimation as the mechanism of nanosecond laser ablation of tungsten under vacuum conditions, *Spectrochim. Acta B* 122, 1 (2016)
40. J. Rapp, W. R. Koppers, H. J. N. van Eck, G. J. van Rooij, W. J. Goedheer, B. de Groot, R. Al, M. F. Graswinckel, M. A. van den Berg, O. Kruyt, P. Smeets, H. J. van der Meiden, W. Vijvers, J. Scholten, M. van de Pol, S. Brons, W. Melissen, T. van der Grift, R. Koch, B. Schweer, U. Samm, V. Philipps, R. A. H. Engeln, D. C. Schram, N. J. L. Cardozo, and A. W. Kleyn, Construction of the plasma-wall experiment Magnum-PSI, *Fusion Eng. Des.* 85(7–9), 1455 (2010)
41. G. De Temmerman, M. A. van den Berg, J. Scholten, A. Lof, H. J. van der Meiden, H. J. N. van Eck, T. W. Morgan, T. M. de Kruijf, P. A. Z. van Emmichoven, and J. J. Zielinski, High heat flux capabilities of the Magnum-PSI linear plasma device, *Fusion Eng. Des.* 88(6–8), 483 (2013)
42. C. Li, X. Wu, C. Zhang, H. Ding, G. De Temmerman, and H. J. van der Meiden, Study of deuterium retention on lithiated tungsten exposed to high-flux deuterium plasma using laser-induced breakdown spectroscopy, *Fusion Eng. Des.* 89(7–8), 949 (2014)
43. K. Piip, G. De Temmerman, H. J. van der Meiden, A. Lissovski, J. Karhunen, M. Aints, A. Hakola, P. Paris, M. Laan, J. Likonen, I. Jõgi, J. Kozlova, and H. Mändar, LIBS analysis of tungsten coatings exposed to Magnum PSI ELM-like plasma, *J. Nucl. Mater.* 463, 919 (2015)
44. P. Paris, A. Hakola, K. Bystrov, G. De Temmerman, M. Aints, I. Jõgi, M. Kiisk, J. Kozlova, M. Laan, J. Likonen, and A. Lissovski, Erosion of marker coatings exposed to Pilot-PSI plasma, *J. Nucl. Mater.* 438, S754 (2013)
45. C. Li, X. Wu, C. Zhang, H. Ding, J. Hu, and G. N. Luo, In situ chemical imaging of lithiated tungsten using laser-induced breakdown spectroscopy, *J. Nucl. Mater.* 452(1–3), 10 (2014)
46. Q. Xiao, R. Hai, H. Ding, A. Huber, V. Philipps, N. Gierse, and G. Sergienko, In-situ analysis of the first wall by laser-induced breakdown spectroscopy in the TEXTOR tokamak: Dependence on the magnetic field strength, *J. Nucl. Mater.* 463, 911 (2015)